May 2014

Averaging improves strain images of the biceps brachii using quasi-static ultrasound elastography

Matthew Leineweber
Cornell University

J Westborn
Cornell University

A Cochran
Cornell University

Y Gao
Cornell University

J Choi
Guthrie Clinic

Recommended Citation

Matthew Leineweber, J Westborn, A Cochran, Y Gao, and J Choi. "Averaging improves strain images of the biceps brachii using quasi-static ultrasound elastography" *British Journal of Radiology* (2014). https://doi.org/10.1259/bjr.20130624

BJR

Received: 1 October 2013 | Revised: 6 March 2014 | Accepted: 22 April 2014

doi: 10.1259/bjr.20130624

Cite this article as:
Leineweber MJ, Westborn J, Cochran A, Choi J, Gao Y. Averaging improves strain images of the biceps brachii using quasi-static ultrasound elastography. Br J Radiol 2014;87:20130624.

FULL PAPER

Averaging improves strain images of the biceps brachii using quasi-static ultrasound elastography

[1]M J LEINEWEBER, MS, [1]J WESTBORN, MEng, [2]A COCHRAN, PhD, [3]J CHOI, MD, PhD and [1]Y GAO, PhD

[1]Mechanical and Aerospace Engineering Department, Cornell University, Ithaca, NY, USA
[2]Department of Mathematics, Cornell University, Ithaca, NY, USA
[3]Guthrie Clinic, Sayre, PA, USA

Address correspondence to: Dr Yingxin Gao
E-mail: *yg75@cornell.edu*

Objective: Quasi-static ultrasound elastography is a technique for measuring tissue deformation (strain) under externally applied loading and can be used to identify the presence of abnormalities. The objective of this study was to demonstrate the efficacy of averaging strain images from repeated compression cycles in mitigating user-induced error using quasi-static ultrasound elastography.
Methods: Freehand compressions were performed with an ultrasound transducer on the biceps brachii of nine participants (five males and four females), as well as with a custom automated compression system. Sets of strain images from the freehand techniques were averaged to create single representative images and compared against strain images from the automated compressions using both qualitative and quantitative metrics.
Results: Significant improvements in intra-operator repeatability and interoperator reproducibility can be achieved by averaging strain images from four to eight repeated compressions. The resulting strain images did not lose significant image data compared with strain images from single automated compressions.
Conclusion: Averaging is introduced as a feasible and appropriate technique to improve strain image quality without sacrificing important image data.
Advances in knowledge: Simple averaging of multiple freehand elastography measures can achieve a similar degree of accuracy, repeatability and reproducibility as that of more awkward and expensive automated methods. The resulting elastograms can be used to obtain a more accurate and complete diagnosis without additional cost to the doctor or the patient.

Damage to the skeletal muscle tissue, such as contusions, tears and strains, accounts for approximately 90% of all sport-related injuries.[1] Although MRI is currently the gold standard for diagnostic imaging of soft tissue, ultrasound is recognized as a viable alternative for soft-tissue imaging, owing to its portability, affordability and ability to capture sequences of images in real time.[2,3] Quasi-static elastography (QSE) takes advantage of the unique ability of ultrasound to capture image sequences to track tissue deformation and has emerged as a potential diagnostic tool to monitor musculoskeletal pathologies.[4]

QSE operates on the principle that when tissue is externally compressed, the resulting deformation depends on the mechanical properties of the tissue.[5] Accordingly, this technique tries to recover information about the mechanical properties from the information about tissue deformation. Ultrasound elastography has been shown to detect lesions in the breast tissue and fibrosis in the liver tissue[6–9] and to measure intravascular elasticity,[10,11] as well as an ability to estimate strain in tendons.[12–14] QSE could also potentially be used to identify regions of damaged or abnormal tissue in skeletal muscles, but there are few studies exploring these applications.[4]

The primary limitation of QSE is its dependence on consistent and steady ultrasound images to create quality strain images. Image steadiness is particularly important with musculoskeletal tissues owing to their anisotropic and inhomogeneous structure. Variability in image collection, inherent to the nature of freehand manipulation of the ultrasound transducer, results in changes in the imaging window and unsteady application of force during a single compression, as well as variations in the rate, magnitude and direction of loading between trials. These inconsistencies may lead to large errors in the resulting strain images, directly affecting the accuracy and repeatability of strain measurements. For example, transducer misalignment alone has been shown to result in strain measurement errors as high as 23%.[15] To mitigate variation

between examinations and measurement error, a number of studies have developed scanning systems that assist the operator while examining the tissue of interest. These automated and assisted systems have employed various mechanical compression and feedback techniques to successfully reduce extraneous transducer motion and improve the resulting strain images.[16–18] However, these enhancements do come at the cost of added training and expensive, often cumbersome equipment.

Rather than attempting to eliminate the aforementioned sources of measurement error themselves, it may be possible to minimize the imprecision of the strain images through a simple averaging procedure, wherein multiple ultrasound compression scans are performed, and the resulting strain images averaged to create a single representative image.

Although averaging is expected to improve repeatability in the strain images, currently, there is no literature employing such averaging techniques to musculoskeletal elastography. Instead, multiple compressions are performed, and the result of a single scan is selected from amongst the set to be further analysed.[13,14,19] Several questions about the approach of averaging need to be addressed, including (1) can it achieve similar strain image repeatability as automated scans? (2) Does it require too many scans to achieve acceptable repeatability? (3) Will averaging actually remove important data in the image that are unique to the patient and are needed to properly characterize the tissue health?

In this article, we determine whether averaging strain images from repeated scans of the biceps brachii reduces the effects of variability in ultrasound images. Specifically, we tested three hypotheses: (1) the final images created by averaging strain images over multiple manual scans are both qualitatively and quantitatively similar to strain images resulting from automated compression procedures; (2) averaging over multiple scans increases the repeatability of the resulting strain images compared with that of single automated compressions; and (3) the averaged strain images from a single subject will be more reproducible between operators than strain images from a single freehand scan.

METHODS AND MATERIALS

All testing procedures were performed with approval from the Cornell University (Ithaca, NY) Institutional Review Board. Nine healthy volunteers (five males and four females) aged 26.4 ± 3.2 [mean $\pm$ standard deviation (SD)] years were recruited from Cornell University. The participants selected were asked to fill out a questionnaire about their health history to ensure that they did not have any history of musculoskeletal diseases or injury to the biceps brachii. All participants underwent ultrasound imaging of the dominant arm biceps brachii. The participants provided informed consent prior to their involvement in the study.

This section details the procedure used to (1) create averaged strain images from multiple compressions of the biceps brachii and (2) test the accuracy (similarity to automated images), repeatability and reproducibility of these averaged images.

Establishing the imaging window

An adjustable armrest was used to maintain consistent positioning of the biceps during the ultrasound scans, as shown in Figure 1. With the arm brought out directly in front of the participant (forming a 90° angle to the shoulders), the posterior surface of the upper arm rested on a pad parallel to the tabletop, and the elbow was flexed to allow the forearm to rest on a pad at 30° from horizontal. The wrist was maintained in a supinated position with neutral flexion. The arm and hand were fully supported, allowing the biceps to remain in a neutral, static position with no muscle activation.

A transducer positioning protocol was followed to orient the transducer at the onset of each compression. During compression, the transducer motion consists of only translation along the beam axis. This constraint is ensured using a combination of external and internal structures (visible in the ultrasound B-mode image) as landmarks to establish proper transducer location and orientation. The transducer was placed on the anterior surface of the upper arm and oriented to visualize the long axis of the muscle fibres with the distal ends of the fibres aligned with the left of the B-mode image (Figure 2). Using the distal biceps tendon as a starting point, the transducer was translated proximally along the midline of the muscle until the central aponeurosis was no longer visible in the B-mode image. The rotational degrees of freedom were constrained using the length, thickness and curvature of the bone line and muscle fibres in the image as markers. The bone line of the humerus was used to indicate the alignment of the transducer with its long axis; any deviations from the axis were seen as increased curvature of the bone line. The brightness and clarity of the line indicated how well the transducer was rotated about the long axis of the humerus. A blurry or otherwise unclear bone line suggested that the imaging window only partially captured the bone, so the rotation about the long axis could be corrected.

The ultrasound imaging used a Terason t3000™ academic ultrasound system with a 3.81-cm (1.5 inches) wide 7.5-MHz

Figure 1. Setup for the positioning of the arm for ultrasound imaging. The upper (solid arrow) and lower (hollow arrow) arms are supported by arm pads to ensure that the biceps are relaxed and held in position. All imaging procedures were performed on the anterior portion of the upper arm as shown.

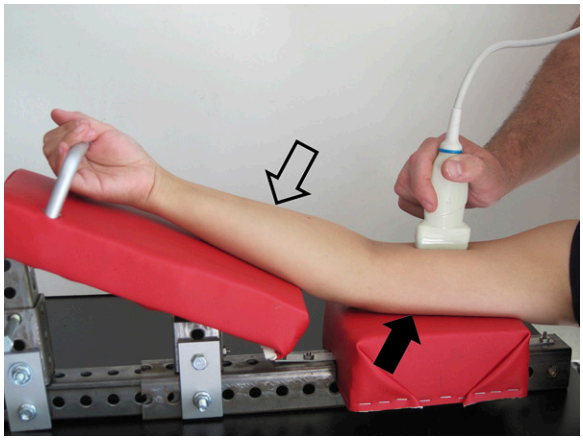

Figure 2. Sonogram of the upper arm with transducer oriented along the muscle fibres. The upper and lower boundaries of the biceps brachii are denoted by single arrows. Double arrows indicate the humerus. The area between the humerus and the lower boundary of the biceps brachii is the brachialis muscle and has not been included in this study.

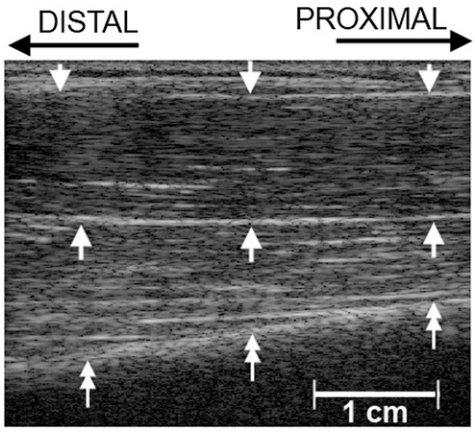

linear array transducer (Teratech Corporation, Burlington, MA) set to image to a depth of 5 cm. The radiofrequency (RF) data were recorded at 30 MHz throughout the compression. These data were represented as B-mode videos of muscle compression transverse to the fibre lengths. The RF data were recorded at approximately 31 frames per second, and the resulting frames were 1948 × 256 pixels (depth × width) in size. Each compression was 3 s in duration, totalling 93 frames collected per compression.

Collecting ultrasound images

All of the ultrasound imaging procedures were performed by a researcher with over 4 years' experience with ultrasound systems and musculoskeletal imaging, as well as by an experienced orthopaedic surgeon.

At the beginning of each freehand compression, the transducer was positioned using the procedures described previously. The operator held the transducer and manually pressed the transducer face against the surface of the arm to compress the muscle tissue (Figure 1). The operator was instructed to apply a slow and steady compression for the 3 s duration.[10,17] After the compression, the video data were examined to determine the frames corresponding to the onset and completion of the compression. This compression procedure was repeated 30 times with a 15-s break being held between scans. This break allows the muscle to recover and ensures that the compressions were independent of each other.

Four of the nine original subjects underwent repeated freehand compressions performed by a clinician during an additional testing session. The scanning protocol was identical to that described above, except 15 compressions were recorded rather than 30.

Automated compressions were conducted using a custom developed mechanical scanner. The scanning apparatus (Figure 3) consisted of a transducer mounted to a one-axis linear actuator (Physik Instrumente (PI) GmbH and Co. KG, Karlsruhe/Palmbach, Germany) connected to a basic motion control system (Arcus Technology ACE-SDE, Livermore, CA). The transducer was positioned according to the aforementioned standard positioning procedure before the first compression, and the positioning was maintained during subsequent scanning procedures. 30 consecutive scans were performed with the scanning system set to compress at 2 mm s^{-1} for 3 s, and the first 5 mm of displacement were recorded.

Creating strain images

The ultrasound raw data were converted into MATLAB® MAT-files (MathWorks®, Natick, MA), using a program provided by Terason® (Burlington, MA).[20] A speckle-tracking algorithm was used to track the motion of small groups of pixels between frames. These motion data were quantified to create a measurement of displacement for each pair of consecutive frames in a B-mode image. The algorithm employed in this study is based on well-developed techniques commonly used in the literature.[20–24]

Figure 3. The automated compression system provided consistent, repeatable compressions to the biceps brachii. The transducer is attached to a motor controlled by the computer. The transducer moved 5 mm.

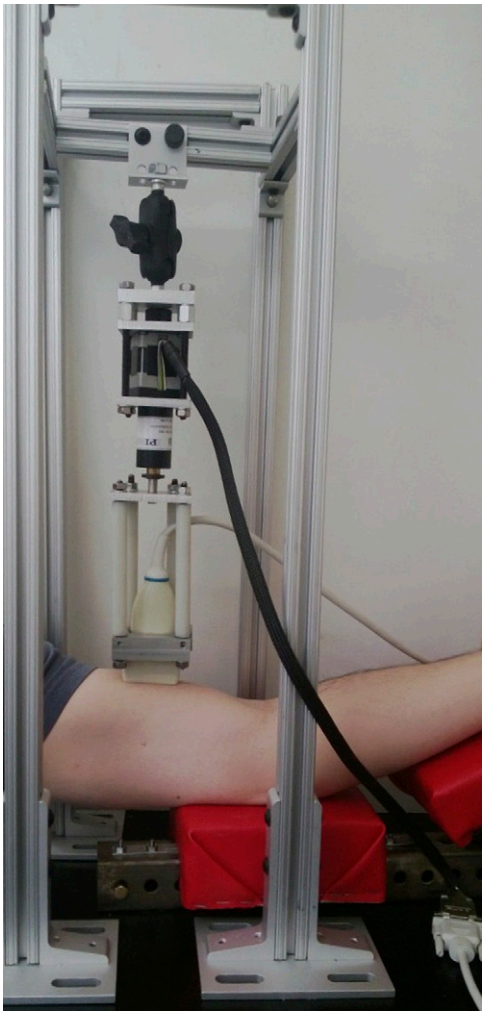

The incremental frame-to-frame strains were accumulated to calculate the total strain over the course of the compression.[10] The first 20 frames of each compression scan were analysed to ensure that the results were drawn from the same segment of the compression. 20 was chosen as the number of frames that experienced sufficient and measurable cumulative strain while allowing for an appropriate computation time.[7] Local strains between consecutive frames were recorded, as were the cumulative strains at each frame relative to the first frame of the 20-frame compression segment.

In the first of the 20 frames selected from each compression, the biceps brachii was manually outlined and selected as the region of interest (ROI). The ROI was defined on its upper and lower boundaries by the interface of the muscle and superficial connective tissue and the interface of the biceps brachii and brachialis, respectively (Figure 2). The left and right boundaries were set approximately 7.5 mm from the edges of the image. Since the deformations were small over the 20-frame selection (approximately 0.065 mm per frame or 1.3 mm over the 20-frame selection), the total change in muscle depth was minimal and the same ROI mask was applied to each frame. Displacements were tracked solely within the ROI. Compression was applied along the ultrasound beam path (transverse to the muscle long axis), and the resolution is highest in this direction as well, thus, only displacements along the beam path were considered for analysis.

The mean compressive strain magnitude was calculated for each cumulative strain image. The strain image from each scan with the mean strain nearest 2% was chosen for averaging. This magnitude-based selection allows for variable compression rates and magnitudes within each 20-frame scan. The cumulative strain image selected from each scan was used in the subsequent averaging procedure.

Averaged strain images for each subject were created from groups of images drawn from each set of 30 scans. Different sized groups were used to determine the minimum number of images necessary for averaging to produce improvements in strain image quality. Thus, the images from each set were divided into groups of 1, 2, 4 and 8 images, for a total of eight groups per set of 30 images (two sets of groups of 1, 2, 4 and 8 images). The images in each group were selected at random without replacement for all groups. Within each group, the averaged strain images were defined by the equation:

$$\text{Image} = \frac{\sum_{i=1}^{n} M\{i\}}{n}$$

For $n = 1$, 2, 4 and 8, and $M\{i\}$ is the strain map corresponding to the "i-th" scan within each group. The strain images were aligned at the upper-left corner, then directly summed. The total summed images were then divided by the number of images included to create the average image. Thus, a total of eight averaged strain images were created from each set of scans.

Quantitative comparison metric

The final averaged images from each subject were compared visually against the strain images from the automated compressions for similarities in strain magnitude, noise levels and strain distribution across the tissue. The mean and SD of the strain magnitudes for the selected automated strain images and each of the averaged images were recorded for all subjects.

Image similarity was defined as the matrix norm of the difference in strain magnitude between any pair of strain images. The strain magnitudes in each image were normalized by the norm of the image. The resulting similarity metric, called the *norm-error*, was calculated as:

$$\text{Norm error} = \left\| \frac{\text{Image}_1}{\|\text{Image}_1\|} - \frac{\text{Image}_2}{\|\text{Image}_2\|} \right\|$$

where $\|x\|$ represents the matrix norm of the resulting image. Smaller values denote a higher degree of similarity between the two images. This metric was used to compare different sets of images depending on the desired outcome measure (image accuracy, repeatability or reproducibility).

Accuracy, repeatability and reproducibility measurements

Strain images from single automated compressions were considered the "gold standard" of image quality. Thus, the accuracy of the averaged images was quantified through comparison of the norm-error values between these gold standard images and the averaged images from two, four, and eight compressions. The norm-error between randomly selected automated strain images was considered the baseline image similarity representing the best of current clinical practice.

Repeatability was defined as the degree of similarity between the pairs of averaged images created using the same number of strain images for each subject. Given the two sets of groups of one, two, four and eight averaged images per set of 30 scans, a total of four repeatability measurements were recorded for each subject. To illustrate, the averaged image created from one group of eight strain images was compared against the averaged image created from the second group of eight images. The resulting norm-error value was designated as the repeatability metric for that subject.

Similarly, reproducibility was quantified as the norm-error value between corresponding images from the two different ultrasound operators (one trained researcher and one clinician). That is, for each of the four subjects scanned by the clinician, the resulting single freehand strain images and averaged images were compared against their counterparts in the original data set.

Statistical analysis

All results are presented as mean ± SD. One-way analysis of variance with Tukey honest significant difference (HSD) *post hoc* test (JMP® Pro v. 10.0; SAS Institute Inc., Cary, NC) were performed on the repeatability measurements for one-, two-, four- and eight-image averages for all nine subjects. The same procedure was used in the comparison of averaged to automated strain images. Differences were considered statistically significant at $p < 0.05$.

Figure 4. (a) A representative strain image resulting from a single automated scan of the biceps brachii overlaid on the ultrasound image of the upper arm. The elastograms are coloured to show the strain magnitude in the compression direction, with red indicating high degrees of deformation and blue indicating little to no deformation. The strain image in (a) shows considerably more local variation compared with (b) the strain image created using an average of four repeated freehand compressions, but the overall strain distribution and magnitudes are very similar. (c) The strain image from an average of four repeated freehand compressions from a second operator (clinician). Again, there is a relatively high degree of qualitative similarity between the strain images. For colour images please see online www.birpublications.org/doi/full/10.1259/bjr.20130624.

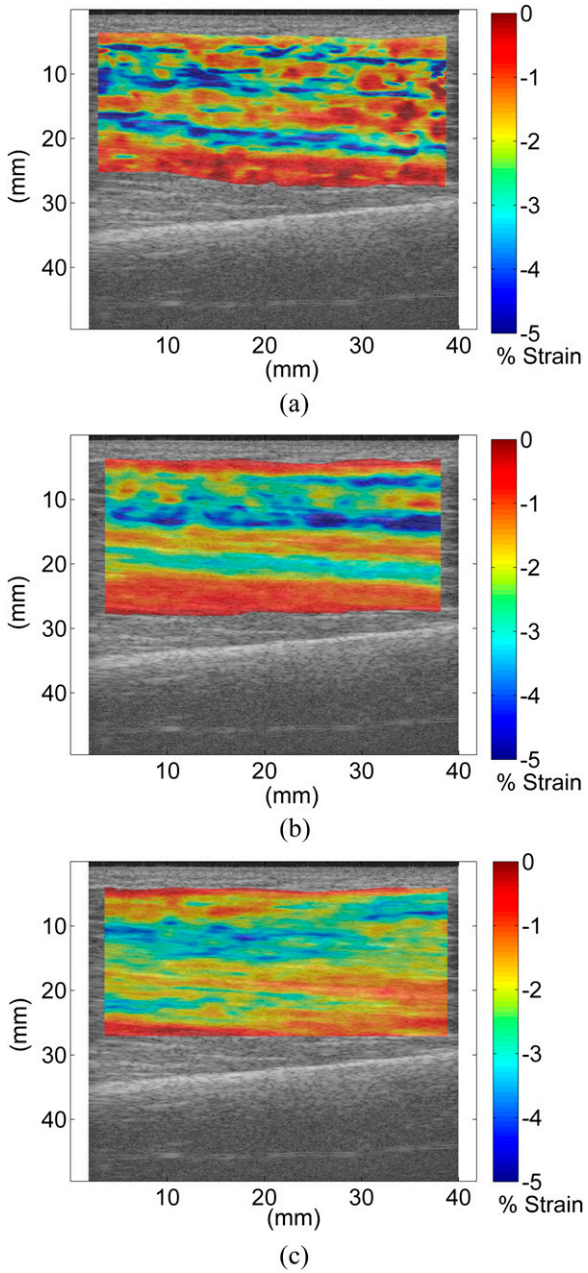

RESULTS

Strain image accuracy

Sample strain images from a single automated compression and an average of four characteristic strain images are shown in Figure 4. While the single automated strain image exhibits a higher degree of local variation, the strain patterns are otherwise visibly similar to the freehand averaged strain image. For a target 2% mean strain, the strain maps exhibit mean strain values of 2.37 ± 0.17% in the averaged images and 2.47 ± 0.84% in the automated images. In general, the single and averaged strain images from each subject followed this trend; comparable overall strain patterns but with less local variability in the averaged images.

The results from the comparison of automated strain images to averaged representative images (Figure 5) show that sets of strain images from automated compressions are as similar to representative images created from averaging as they are to other automated images. The mean norm-error between pairs of automated strain images was not significantly different than the mean norm-error between automated strain images and the averaged representative images.

Repeatability

The results of the repeatability measurements are illustrated in Figure 6. Smaller norm-error values indicated higher degrees of image similarity. The single image column in the plot refers to the similarity of pairs of single strain images resulting from automated compressions of the muscle tissue. The Average 4 and Average 8 groups showed significantly lower norm-error values ($p < 0.05$) than the single image, indicating increased repeatability compared with automated compressions. Mean norm-error values overall tended to decrease with increasing numbers of

Figure 5. The norm-error between pairs of automated strain images, of automated strain images and an average of four repeated freehand strain images and of automated strain images and an average of eight repeated freehand strain images are shown for all nine subjects. There are no significant differences ($p = 0.05$) in the mean norm-error for any of the columns. This similarity indicates that the averaged images were just as similar to the gold standard automated images as these automated images were to each other, indicating minimal data loss owing to averaging.

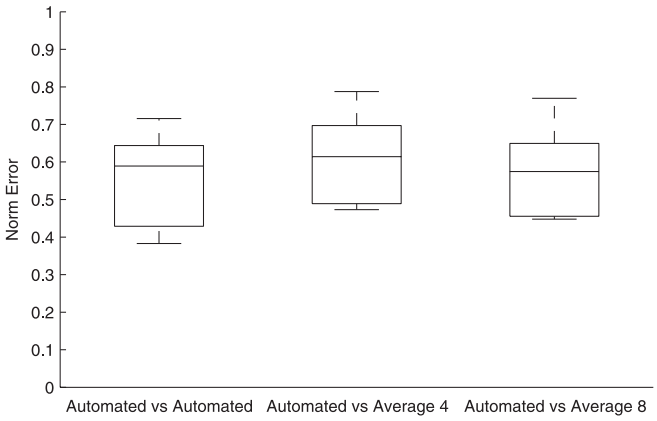

Figure 6. The norm-error between pairs of strain images from each type of strain image is shown for all participants. Significant differences are seen between the single and the Average 4 and Average 8 groups (*). The Average 8 group also exhibited significantly different norm-error values than the Average 2 group ($) but was not different from the Average 4 group. All differences were considered significant at $p < 0.05$.

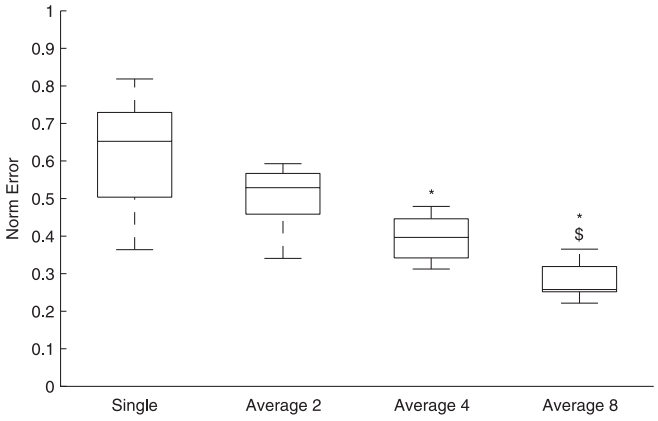

characteristic images included in the averaged representative image. Although the mean norm-error values for the Average 4 and Average 8 groups were not statistically different from each other, both exhibited significantly decreased error values compared with the Average 2 group.

Reproducibility

All three averaging groups exhibited improved interuser reproducibility between representative images than strain images created from two single freehand compressions. However, increasing the number of images in the average from two to eight did not significantly decrease the interuser norm-error values, as can be seen in Figure 7. The decreased norm-error values of the three averaging groups compared with the single group indicate a higher degree of image similarity between users when averaging is used than when single freehand scans are used alone.

DISCUSSION

QSE methods were used to create strain images of the biceps brachii of nine subjects undergoing freehand compression with the ultrasound transducer. The strain images from repeated compressions of a single subject were averaged to create the final averaged image. These averaged strain images exhibited significant improvements in intrasubject repeatability, as well as interoperator reproducibility while remaining qualitatively and quantitatively similar to strain images created using automated compression techniques.

Unsteadiness or variability during the compression stage of QSE has been shown to be a major source of error in the resulting strain images.[18,25] Several groups have attempted to address this issue through the use of automated or semi-automated compression techniques that help remove the "human factor" from the process.[12,17,18] These attempts have successfully shown improvements in displacement tracking and strain image quality. The averaging procedure we describe achieves similar strain image quality using traditional freehand compression techniques.

Figure 7. The norm-error between pairs of corresponding strain images resulting from the two operators. Averaging two or more images decreases the norm-error compared with single freehand scans, indicating an increase in reproducibility between the two operators. There were no significant decreases in norm-error with an increasing number of averaged images from two to eight. ***Significant difference from single freehand scans at $p < 0.001$.

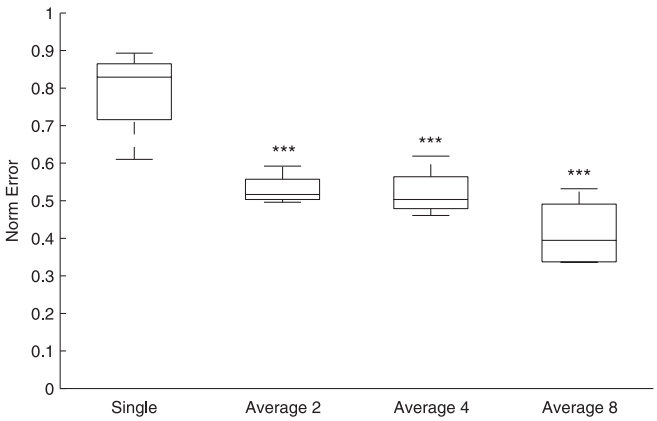

Whereas the automated systems from the aforementioned studies require additional machinery or training to improve the strain images, a simple average of repeated compressions yields qualitatively similar strain images without the extra cost of automated systems.

Not only does averaging produce similar strain images to those from automated compressions, but it improves image repeatability as well. Both the Average 4 and Average 8 groups evidenced increased intrasubject image similarity compared with the single automated group as well as the Average 2 group. This increase in intrasubject image similarity, or repeatability, is indicative of the decrease in noise and error in the strain images. Without the local variations prevalent in strain images from single automated scans, the averaged images are less cluttered with minimal artefacts, and the true strain patterns are more apparent.

In general, the results indicate that increasing the number of images included in the average corresponded to an increase in repeatability. This increase in image similarity is most likely owing to the random noise in the images being smoothed by the higher degree of averaging. Since there was no significant decrease in norm-error moving from the Average 4 group to Average 8 group, the majority of the noise in the strain images is eliminated by including as little as four images in the average.

Variations in operator compression technique or transducer motion can lead to significant noise or artefacts in the resulting strain image. For an accurate diagnosis, these sorts of interoperator variations need to be addressed. The results of this study indicate that averaging can be used to decrease this interoperator error by averaging strain images from as few as two repeated compressions. Similar to repeatability, the increased reproducibility is most likely owing to the smoothing of the local strain magnitude fluctuations seen in strain images from single compressions.

The qualitative and quantitative similarities between the single strain images and averaged strain images indicate that averaging did not eliminate important image information.

Averaging strain images from repeated compressions has the additional advantage that it can be employed regardless of the compression technique. Improvements in freehand compression techniques or automated compressions can be further enhanced through the addition of averaging. Although there may be extra time required for performing multiple scans, current clinical practice often selects the "best" or most representative strain image from a set of three to five compressions.[13,14,19] Since four strain images are all that are needed to see an improvement in the strain image consistency, there is no additional time cost associated with image acquisition using averaging.

It should be noted that for any form of tissue compression, proper transducer positioning and alignment is absolutely necessary for elastography to be effective. Changes in imaging window directly affect the speckle tracking and subsequent displacement images regardless of the compression type. For scans in this study, care was taken to achieve consistent imaging windows at the onset of compression, while minimizing transducer sliding and out-of-plane motion during scanning to ensure accurate and representative strain images.

QSE is a highly operator-dependent technique with subjective results that make comparison between operators, patients and experimental results difficult. As such, this technique is widely regarded as qualitative in nature, and any attempts at quantitative analysis have required specialized compression setups or specific imaging windows, which are not standard.[13,26,27] In this article, we employed a norm-error measurement to attempt to quantify overall image similarity between pairs of strain images. However, this metric alone cannot be used to identify the presence or absence of key strain patterns or expected image features that may be distinctive of the specific tissue (in this case, muscle) being analysed. Our norm-error metric does provide important information on image similarity but must be used in conjunction with qualitative assessment of the strain images in question.

The primary limitation of this study arises from a lack of standard practice for comparing strain images. While some tissues, such as the breast tissue, have been studied in some depth, and some common patterns have been linked to the presence of tumours or abnormal tissue, skeletal muscle elastography has not been explored in sufficient detail to definitively identify strain patterns corresponding to healthy tissue, let alone injured or abnormal tissue. Future work will begin to characterize common strain patterns in healthy and abnormal muscle tissue and to develop more comprehensive image comparison techniques to quantify the degree of abnormality. For example, a more complete comparison between strain images might employ image feature detection and image comparison algorithms to identify expected strain patterns within the tissue.

CONCLUSION

Averaging is introduced as a feasible and appropriate technique to improve ultrasound elastography of the skeletal muscle. Creating an average image from a series of repeated tissue compression cycles leads to increased intrasubject strain image repeatability and reproducibility compared with strain images resulting from automated compressions, while achieving qualitatively and quantitatively similar strain patterns. The authors recommend using strain data from four to eight repeated compressions to create the final average image. This number of repeated compressions is similar to that already employed in clinical practice, thereby resulting in improved final strain image quality without requiring significant additional effort by the operator. Averaging may be an ideal tool to improve the final strain image quality, and ultimately the diagnostic power of QSE of muscle tissue, without the cost of additional machinery.

REFERENCES

1. Beiner JM, Jokl P, Cholewicki J, Panjabi MM. The effect of anabolic steroids and corticosteroids on healing of muscle contusion injury. *Am J Sports Med* 1999; **27**: 2–9.
2. Campbell SE, Adler R, Sofka CM. Ultrasound of muscle abnormalities. *Ultrasound Q* 2005; **21**: 87–94.
3. Martinson H, Stokes MJ. Measurement of anterior tibial muscle size using real-time ultrasound imaging. *Eur J Appl Physiol Occup Physiol* 1991; **63**: 250–4.
4. Drakonaki EE, Allen GM, Wilson DJ. Ultrasound elastography for musculoskeletal applications. *Br J Radiol* 2012; **85**: 1435–45. doi: 10.1259/bjr/93042867.
5. Sarvazyan A, Hall TJ, Urban MW, Garra BS. An overview of elastography-an emerging branch of medical imaging. *Curr Med Imaging Rev* 2012; **7**: 255–82.
6. Ginat DT, Destounis SV, Barr RG, Castaneda B, Strang JG, Rubens DJ. US elastography of breast and prostate lesions. *Radiographics* 2009; **29**: 2007–16. doi: 10.1148/rg.297095058
7. Hiltawsky KM, Kruger M, Ermert H, Jensen A. Freehand ultrasound elastography of breast lesions: clinical results. *Ultrasound Med Biol* 2001; **27**: 1461–9.
8. Ophir J, Cespedes I, Garra B, Ponnekanti H, Huang Y, Maklad N. Elastography: ultrasonic imaging of tissue strain and elastic modulus in vivo. *Eur J Ultrasound* 1996; **3**: 49–70.
9. Friedrich-Rust M, Ong M-F, Herrmann E, Dries V, Samaras P, Zeuzem S, et al. Real-time elastography for noninvasive assessment of liver fibrosis in chronic viral hepatitis. *Am J Roentgenol* 2007; **188**: 758–64. doi: 10.2214/AJR.06.0322
10. Doyley MM, Bamber JC, Fuechsel F, Bush NL. A freehand elastographic imaging approach for clinical breast imaging: system development and performance evaluation. *Ultrasound Med Biol* 2001; **27**: 1347–57.
11. De Korte C, Pasterkamp G, van der Steen A, Woutman H, Bom N. Characterization of plaque components with intravascular ultrasound elastography in human femoral and coronary arteries in vitro. *Circulation* 2000; **102**: 617–23.
12. Varghese T, Zagzebski J, Frank G, Madsen EL. Elastographic imaging using a handheld

compressor. *Ultrason Imaging* 2002; **24**: 25–35.
13. Drakonaki EE, Allen GM, Wilson DJ. Real-time ultrasound elastography of the normal Achilles tendon: reproducibility and pattern description. *Clin Radiol* 2009; **64**: 1196–202. doi: 10.1016/j.crad.2009.08.006
14. De Zordo T, Fink C, Feuchtner GM, Smekal V, Reindl M, Klauser AS. Real-time sonoelastography findings in healthy Achilles tendons. *Am J Roentgenol* 2009; **193**: W134–8. doi: 10.2214/AJR.08.1843
15. Rana M, Wakeling JM. In-vivo determination of 3D muscle architecture of human muscle using free hand ultrasound. *J Biomech* 2011; **44**: 2129–35. doi: 10.1016/j.jbiomech.2011.05.026
16. Hall TJ, Zhu Y, Spalding CS. In vivo real-time freehand palpation imaging. *Ultrasound Med Biol* 2003; **29**: 427–35.
17. Han L, Noble JA, Burcher M. A novel ultrasound indentation system for measuring biomechanical properties of in vivo soft tissue. *Ultrasound Med Biol* 2003; **29**: 813–23.
18. Kadour MJ, Noble JA. Assisted-freehand ultrasound elasticity imaging. *IEEE Trans Ultrason Ferroelectr Freq Control* 2009; **56**: 36–43.
19. Bhatia KS, Rasalkar DD, Lee Y-P, Wong K-T, King AD, Yuen Y-H, et al. Real-time qualitative ultrasound elastography of miscellaneous non-nodal neck masses: applications and limitations. *Ultrasound Med Biol* 2010; **36**: 1644–52. doi: 10.1016/j.ultrasmedbio.2010.07.010
20. Cochran AL, Gao Y. An ultrasound elastography method for examining the anterior cruciate ligament. *Nat Sci* 2013; **5**: 23–31.
21. Pesavento A, Member S, Perrey C, Krueger M, Ermert H, Member S. A time-efficient and accurate strain estimation concept for ultrasonic elastography using iterative phase zero estimation. *IEEE Trans Ultrason Ferroelectr Freq Control* 1999; **46**: 1057–67.
22. Chen H, Shi H, Varghese T. Improvement of elastographic displacement estimation using a two-step cross-correlation method. *Ultrasound Med Biol* 2007; **33**: 48–56.
23. Chen L, Housden RJ, Treece GM, Gee AH, Prager RW. A hybrid displacement estimation method for ultrasonic elasticity imaging. *IEEE Trans Ultrason Ferroelectr Freq Control* 2010; **57**: 866–82. doi: 10.1109/TUFFC.2010.1491
24. Maher C, Baessler K, Glazener CM, Adams EJ, Hagen S. Surgical management of pelvic organ prolapse in women. *Cochrane Database Syst Rev* 2004: CD004014.
25. Chandrasekhar R, Ophir J, Krouskop T, Ophir K. Elastographic image quality vs. tissue motion in vivo. *Ultrasound Med Biol* 2006; **32**: 847–55. doi: 10.1016/j.ultrasmedbio.2006.02.1407
26. Niitsu M, Michizaki A, Endo A, Takei H, Yanagisawa O. Muscle hardness measurement by using ultrasound elastography: a feasibility study. *Acta Radiol* 2011; **52**: 99–105. doi: 10.1258/ar.2010.100190
27. Park G-Y, Kwon DR. Application of real-time sonoelastography in musculoskeletal diseases related to physical medicine and rehabilitation. *Am J Phys Med Rehabil* 2011; **90**: 875–86. doi: 10.1097/PHM.0b013e31821a6f8d